TECHNICAL PAPER

Generalized diffusion effects on Maxwell nanofluid stagnation point flow over a stretchable sheet with slip conditions and chemical reaction

Mair Khan[1] · M. Y. Malik[1,3] · T. Salahuddin[2] · Farzana Khan[1]

Abstract

The aim of this article is to investigate the heat and mass diffusion (Cattaneo–Christov model) of the upper convected Maxwell nanomaterials passed by a linear stretched surface (slip surface) near the stagnation point region. Convocational Fourier's and Fick's laws are employed to investigate heat and mass diffusion phenomena. Using the similarity transformations, the governing PDEs are rendered into ODEs along with boundary conditions. The boundary value problem is solved numerically using RK-4 method along with shooting technique (Cash and Karp). The effects of embedded parameters, namely fluid relaxation parameter, Hartmann number, Brownian moment, thermophoresis parameter, thermal relaxation parameter, Lewis number, chemical reactions concentration relaxation parameter, and slip parameter on velocity, temperature, and concentration distributions, are deliberated through the graphs and discussed numerically. The skin friction coefficient is deliberated numerically, and their numerical values are accessible through graphs and table. The comparison of current article is calculated in the last section, and a good agreement is clear with the existing literature.

1 Introduction

Nanotechnology has important interest in manufacturing, aerospace, and medical industries. The term nanofluid was generated by Choi [1] in 1995, designated as fluids that contain solid nanoparticles having 1–100 nm size dispersed in the base fluids, namely ethylene, water, toluene, oil, etc. Nanoparticles such as coppers, silicone, aluminum, and titanium tend to improve the thermal conductivity and convective heat assignment rate of liquids. Impact of variable viscosity on flow of non-Newtonian material with convective conditions over a porous medium is investigated by Rundora et al. [2]. Babu and Sandeep [3] discussed the numerical solution on MHD nanomaterials over a variable thickness of the surface along with thermophoresis and Brownian motion effects. Haiao [4] presented the numerical solution of magnetohydrodynamic micropolar fluid flow with the addition of nanomaterials toward a stretching sheet with viscous dissipation. Mahdavi et al. [5] illustrated the slip velocity along with multiphase approach of nanofluids. Xun et al. [6] obtained the numerical solution of bioconvection heat flow nanofluid flow over a rotating plate with temperature-based viscosity. Khan et al. [7] numerically analyzed heat and mass diffusion in Jeffery nanofluid passed by inclined stretching surface. Lebon and Machrafi [8] analyzed the two-phase change in Maxwell nanofluid flow along with thermodynamic description. Ansari et al. [9] investigated the comprehensive analysis in order to calculate the relative viscosity of nanofluids. Khan et al. [10] considered the chemical reaction on Carreau–Yasuda nanomaterials over a nonlinear stretching surface.

Magnetohydrodynamic (MHD) flow of heat and mass transfer Maxwell fluid flow over a continuous stretching surface has

---

Technical Editor: Cezar Negrao, Ph.D.

✉ Mair Khan
  mair.khan@math.qau.edu.pk

1 Department of Mathematics, Quaid-i-Azam University, Islamabad 44000, Pakistan

2 Department of Mathematics, Mirpur University of Science and Technology (MUST), Mirpur 10250, Pakistan

3 Department of Mathematics, College of Sciences, King Khalid University, Abha 61413, Saudi Arabia

great significance in several applications in engineering such as melts, aerodynamics extrusion of plastic sheet, geothermal extractions, and purification of molten metals. Numerous researchers have made great interest and evaluated the transport phenomena for magnetohydrodynamic. Zhao et al. [11] solve the differential equations labeling MHD Maxwell fluid in permeable sheet by considering Dufour and Soret impact. Hsiao [12] investigated the combined effects of thermal extraction on MHD Maxwell fluid over stretching surface with viscous dissipation and energy conversion. Ghasemi and Siavashi [13] demonstrated the Cu–water MHD nanofluid in square permeable surface with entropy generation. Nourazar et al. [14] illustrated the heat transfer in flow of single-phase nanofluid toward a stretching cylinder with magnetic field effect. Dogonchi and Ganji [15] addressed the unsteady squeezed MHD nanofluid flow over two parallel plates with solar radiation. Hayat et al. [16] investigated the heat and mass diffusion for stagnation point flow toward a linear stretching surface along with magnetic field. Sayyed et al. [17] investigated the analytical solution of MHD Newtonian fluid flow over a wedge occupied in a permeable sheet. Representative analyses on MHD flow can be seen in Refs. [18–20].

The Maxwell model is a subclass of rate-type fluids, which calculates stress relaxation so it has become popular. This model also eliminates the complicating behavior of shear-dependent viscosity and is thus useful for focusing exclusively on the impact of a fluid's elasticity on the characteristics of its boundary layer. Nadeem et al. [21] deliberated the numerical study on heat transfer of Maxwell nanofluid flow over a linear stretching sheet. Reddy et al. [22] studied the approximate solution of magnetohydrodynamic Maxwell nanofluid flow over exponentially stretching surface. Liu [23] indicated the 2D flow of frictional Maxwell fluid over a variable thickness. Solution of the differential equations was obtained numerically here by L_1 technique. Yang et al. [24] considered the fractional Maxwell fluid through a rectangular microchannel.

Inspired by the above studies, the current study illustrates the MHD Maxwell nanofluid flow over a linearly stretched sheet near the stagnation point and slip boundary conditions. Fourier's and Fick's laws are presented in the constitutive relations. The nonlinear ODEs are deduced from the nonlinear PDEs by similarity transaction. The solutions are obtained via shooting method (Cash and Karp). The different involved physical parameters are examined for velocity, concentration, and temperature fields.

2 Mathematical formulation

Let us consider two-dimensional laminar steady heat and mass transfer flow of an electrically conducting Maxwell nanofluid flow passed by a linear stretched surface placed

along x-axis and y-axis vertical to the sheet with stagnation point at the origin (as illustrated in Fig. 1). The free stream velocity $\mathbf{u} = \mathbf{u}_e(\mathbf{x}) = \mathbf{cx}$ and the velocity via which sheet is stretched are $\mathbf{u} = \mathbf{U}_w(\mathbf{x}) = \mathbf{ax}$, where a and c are positive constants. The temperature at the surface is conserved at T_w and T_∞ far away from the plate; in similar a manner, the nanoparticle volume fractions are C_w and C_∞. An external magnetic field H_0 is applied normal to the sheet.

Under the above assumptions, the required equations are as follows:

$$\frac{\partial u}{\partial x} + \frac{\partial v}{\partial y} = 0, \tag{1}$$

$$u\frac{\partial u}{\partial x} + v\frac{\partial u}{\partial y} + \lambda\left[u^2\frac{\partial^2 u}{\partial x^2} + v^2\frac{\partial^2 u}{\partial y^2} + uv\frac{\partial^2 u}{\partial x \partial y}\right]$$
$$= -\frac{1}{\rho}\frac{\partial P}{\partial x} + v\frac{\partial^2 u}{\partial y^2} - \frac{\sigma\mu_e^2 H_0^2}{\rho}\left(u + \lambda v\frac{\partial u}{\partial y}\right), \tag{2}$$

where ρ is the density, μ_e is the magnetic permeability velocity, σ is the electrical conductivity, λ is the Maxwell fluid parameter, and v is the kinematic viscosity. Due to hydrostatic and magnetic pressure gradient, the force will be in equilibrium as given by

$$-\frac{1}{\rho}\frac{\partial P}{\partial x} = u_e\frac{du_e}{dx} + \frac{\sigma\mu_e^2 H_0^2}{\rho}u_e \tag{3}$$

Hence, Eq. (2) becomes

$$u\frac{\partial u}{\partial x} + v\frac{\partial u}{\partial y} + \lambda\left[u^2\frac{\partial^2 u}{\partial x^2} + v^2\frac{\partial^2 u}{\partial y^2} + uv\frac{\partial^2 u}{\partial x \partial y}\right]$$
$$= u_e\frac{du_e}{dx} + v\frac{\partial^2 u}{\partial y^2} - \frac{\sigma\mu_e^2 H_0^2}{\rho}\left(u - u_e + \lambda v\frac{\partial u}{\partial y}\right). \tag{4}$$
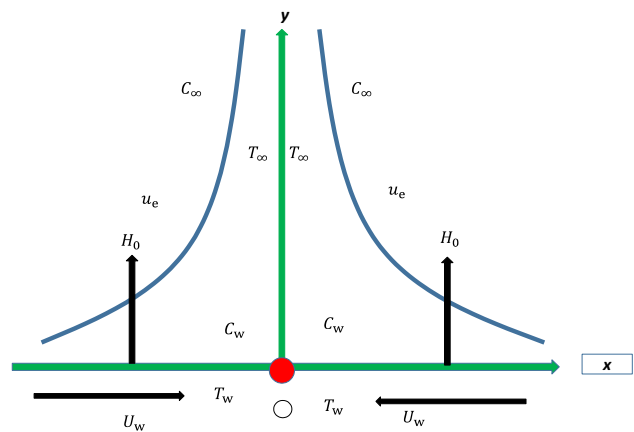

Fig. 1 Geometry of the problem

The classical form of Fourier's and Fick's laws with the ray of Cattaneo–Christov equations takes the following form:

$$q + \lambda_T \left[\frac{\partial q}{\partial t} + V.(\nabla q) - q.(\nabla V) + (\nabla.V)q \right] = -k_f \nabla T, \quad (5)$$

$$J + \lambda_c \left[\frac{\partial J}{\partial t} + V.(\nabla J) - J.(\nabla V) + (\nabla.V)J \right] = -D_B \nabla C. \quad (6)$$

Assume that $\nabla.q = 0$, $\nabla.J = 0$, and for steady state $\frac{\partial q}{\partial t} = 0$, $\frac{\partial J}{\partial t} = 0$, the new equations become:

$$q + \lambda_T [V.\nabla q - q.\nabla V] = -k_f \nabla T, \quad (7)$$

$$J + \lambda_C [V.\nabla J - q.\nabla J] = -D_B \nabla C. \quad (8)$$

Now in component form, energy and concentration Eqs. (7) and (8) take the following form:

$$
\begin{aligned}
& u\partial_x T + v\partial_y T + \lambda_T \left[\partial_x T u (\partial_x u) + \partial_x T v (\partial_y u) \right. \\
& \quad \left. + u(\partial_x v)\partial_y T + v(\partial_y v)\partial_y T \right] \\
& \quad + \lambda_T \left[2uv\partial_{xy} T + v^2 \partial_{yy} T + u^2 \partial_{xx} T \right] \\
& = \alpha \partial_{yy} T + \tau \left\{ D_B (\partial_y T \partial_y C) + \frac{D_T}{T\infty} (\partial_y T)^2 \right\},
\end{aligned}
\quad (9)
$$

$$
\begin{aligned}
& u(\partial_x C) + v(\partial_y C) + \lambda_c \left[u\partial_x u (\partial_x C) + v\partial_y u (\partial_x C) \right. \\
& \quad \left. + u(\partial_x v)\partial_y C + v(\partial_y v)\partial_y C \right] \\
& \quad \lambda_c \left[+2uv\partial_{xy} C + v^2 \partial_{yy} C + u^2 \partial_{xx} C \right] \\
& = D_B \partial_{yy} C + \frac{D_T}{T\infty} \partial_{yy} T - K_1 (C - C_\infty),
\end{aligned}
\quad (10)
$$

where $\partial_x = \frac{\partial}{\partial x}$ and $\partial_y = \frac{\partial}{\partial y}$.

The specified boundary conditions of the current problem take the form

$$\mathbf{u}(\mathbf{x}, \mathbf{y}) = \mathbf{U}_w(\mathbf{x}) = \mathbf{a}x + g\frac{\partial u}{\partial y}, \quad v(x, y) = 0,$$

$$T(x, y) = T_w(x) = T_\infty + bx, \quad C(x, y) = C_w = C_\infty + bx, \text{ at } y = 0,$$

$$\mathbf{u}(\mathbf{x}, \mathbf{y}) = \mathbf{u}_e(\mathbf{x}) = \mathbf{c}x, T(x, y) = T_\infty, C(x, y) = C_\infty \text{ as } y \to \infty. \quad (11)$$

Here (u, v) are the velocity components along the (x, y) directions, q, J are the normal heat and mass flux, respectively, k_f represents the thermal conductivity, D_B is the Brownian motion, λ_T, λ_C are the relaxation parameters for thermal and concentration, $\alpha_f = \frac{(\rho c)_s}{(\rho c)_f}$ is the ratio of nanoparticle heat capacity to base fluid thermal capacity, $\alpha_f = \frac{k_f}{(\rho C_p)_f}$ represents thermal diffusion, $T_w(x, y)$ is known as temperature at the wall, $C_w(x, y)$ is known as concentration at the wall, T and C are the temperature and concentration of the fluid, respectively, C_p is the specific heat, and

C_∞ and T_∞ are the concentration and temperature free streams. Temperature of the sheet is $T_w = T_\infty + bx$, for heated surface $b > 0$ so $T_w > T_\infty$ and for cooled surface $b < 0$ and $T_w < T$, where b is a constant and D_T is known as thermophoresis diffusivity.

Considering the similarity transformations, we have

$$\eta = y\sqrt{\frac{a}{\nu}}, \quad \theta(\eta) = \frac{T - T_\infty}{T_w - T_\infty}, \quad \phi(\eta) = \frac{C - C_\infty}{C_w - C_\infty}, \quad u = \frac{\partial \psi}{\partial y}, \quad v = -\frac{\partial \psi}{\partial x}. \quad (12)$$

Substituting Eq. (12) into Eqs. (1), (4), (9), (10), the present problem boundary conditions (11) are as follows:

$$
\begin{aligned}
& \frac{d^3 f}{d\eta^3} + \frac{df}{d\eta}\frac{d^2 f}{d\eta^2} - \left(\frac{df}{d\eta}\right)^2 + \lambda_m \left(2f(\eta)\frac{df}{d\eta}\frac{d^2 f}{d\eta^2} - (f(\eta))^2 \frac{d^3 f}{d\eta^3} \right) \\
& + Ha^2 \left(1 - \frac{df}{d\eta} + \lambda_m \frac{df}{d\eta}\frac{d^2 f}{d\eta^2} \right) + 1 = 0,
\end{aligned}
\quad (13)
$$

$$
\begin{aligned}
& \frac{d^2 \theta}{d\eta^2} + Pr \left[f(\eta)\frac{d\theta}{d\eta} + N_b \frac{d\varphi}{d\eta}\frac{d\theta}{d\eta} + N_t \left(\frac{d\theta}{d\eta}\right)^2 \right. \\
& \left. + \delta_t \left(f(\eta)\frac{df}{d\eta}\frac{d\theta}{d\eta} - \frac{d^2 \theta}{d\eta^2}(f(\eta))^2 \right) \right] = 0,
\end{aligned}
\quad (14)
$$

$$
\begin{aligned}
& \frac{d^2 \phi}{d\eta^2} + \frac{N_t}{N_b}\frac{d^2 \theta}{d\eta^2} + PrLe \left[f(\eta)\frac{d\phi}{d\eta} - K\phi(\eta) \right. \\
& \left. + \delta_c \left(f(\eta)\frac{df}{d\eta}\frac{d\phi}{d\eta} - \frac{d^2 \phi}{d\eta^2}(f(\eta)^2) \right) \right] = 0.
\end{aligned}
\quad (15)
$$

Using (11), the associated boundary conditions become

$$\frac{df}{d\eta} = 1 + k\frac{d^2 f}{d\eta^2}, \quad f(\eta) = 0, \theta(\eta) = 1, \quad \phi(\eta) = 1, \text{ at } \eta = 0,$$

$$\frac{df}{d\eta} \to A, \quad \theta \to 0, \quad \phi \to 0, \text{ as } \eta \to \infty. \quad (16)$$

where the fluid relaxation parameter is $\lambda_m = \lambda a$, Hartmann number is $Ha^2 = \mu_e H_0 \sqrt{\frac{\sigma}{\rho a}}$, concentration relaxation parameter is $\delta_c = a\lambda_C$, ratio parameter is $A = \frac{c}{a}$, Lewis number is $Le = \frac{\alpha}{D_B}$, thermal relaxation parameter is $\delta_t = a\lambda_T$, thermophoresis parameter is $N_t = \frac{\tau D_t (T_w - T_0)}{T_\infty \nu}$, Prandtl number is $Pr = \frac{\mu c_p}{k}$, Brownian motion parameter is $N_b = \frac{\tau D_B (C_w - C_0)}{\nu}$, slip parameter is $\mathbf{k} = \mathbf{g}\sqrt{\frac{a}{\nu}}$, and chemical reactive species is $K = \frac{K_1}{a}$.

Friction factor coefficient (C_f) is defined as:

$$C_f = \frac{\tau_w}{\rho u_e^2} = Re_x^{\frac{-1}{2}} (f''(0) + \lambda_m(f''(0)f'(0) + f(0)f'''(0))).$$

(17)

Here τ_w denotes the wall shear stress and is given by

$$\tau_w = \mu \frac{\partial}{\partial y}(u + \lambda v \frac{\partial u}{\partial y})_{y=0}.$$

(18)

where $Re_x = u_e x \frac{x}{v}$ is local Reynolds number.

3 Numerical procedure

Numerical solution of the nonlinear differential Eqs. (13)–(15) along with Neumann boundary conditions (16) is achieved by applying the shooting method with RK-4 integration technique for various values of parameters. Let $y_1 = f$, $y_2 = f'$, $y_3 = f''$, $y_4 = \theta$, $y_5 = \theta'$, $y_6 = \phi$ and $y_7 = \phi'$.

Hence, the leading equations become

$$y_1 = y_2',$$

(19)

$$y_2' = y_3,$$

(20)

$$y_3' = \frac{y_2^2 - y_2 y_3 - \lambda_m(y_1 y_2 y_3) - Ha^2(1 - y_2 + \lambda_m y_2 y_3) - 1}{(1 - \lambda_m y_1)},$$

(21)

$$y_4' = y_5,$$

(22)

$$y_5' = \frac{-Pr\left(y_1 y_5 + N_b y_7 y_5 + N_t(y_5)^2 + \delta_t(y_2 y_1 y_5)\right)}{\left(1 - \delta_t(y_1)^2\right)},$$

(23)

$$y_6' = y_7,$$

(24)

$$y_7' = \frac{-PrLe\left(y_1 y_6 - Ky_6 + \delta_c(y_2 y_1 y_6)\right) - \frac{N_t}{N_b} y_5'}{\left(1 - \delta_c(y_1)^2\right)},$$

(25)

and subsequent initial conditions are:

$$y_1(0) = 0, \quad y_2(0) = 1 + ky_2, \quad y_4(0) = 1, \quad y_6(0) = 1,$$
$$y_2(\eta) \rightarrow A, \quad y_4(\eta) \rightarrow 0, \quad y_6(\eta) \rightarrow 0 \text{ when } \eta \rightarrow \infty.$$

(26)

This technique is successfully used to solve the different problems related to boundary layer flows. The boundary conditions $f'(0)$, $\theta(0)$ and $\phi(0)$ for $\eta \rightarrow \infty$ are converted into finite interval length (here it is $\eta = 5$). Insert

three initial guesses to $f''(0)$, $\theta'(0)$ and $\phi'(0)$ for approximate solution. Here the step size and convergence criteria are chosen to be 0.001 and 10^{-6} (in all cases).

4 Results and discussion

The main effort of this work is to examine the influence of magnetic field and stagnation point Maxwell nanofluid flow due to a linear stretching surface with slip conditions. The governing differential Eqs. (12)–(15) along with corresponding boundary conditions (16) are solved numerically by implying shooting procedure (Cash and Karp). Figure 2 represents the change in velocity profile for distinct values of Hartmann number Ha. From this figure, the enhancement in Ha results in decrease in velocity profile. Since the Hartmann number Ha represents the ratio of MHD force to viscous force, the enhancement in Ha leads to stronger the MHD force, which declares the velocity motion. Figure 3 depicts the variation of slip parameter k on velocity profile. The influence of slip parameter k significantly enhances the velocity profile. Figure 4 illustrates the variation of fluid relaxation parameter λ_m on velocity profile. It can be analyzed that the velocity of the fluid reduces by enhancing the fluid relaxation parameter λ_m. Figure 5 represents the change in temperature distribution for distinct values of N_t. It is found that by enhancing N_t, the temperature distribution also increases. Figure 6 depicts the variation of Brownian motion N_b on temperature distribution. It can be analyzed that by increasing N_b, the mass diffusivity trekked up which leads to enhancement in the temperature and
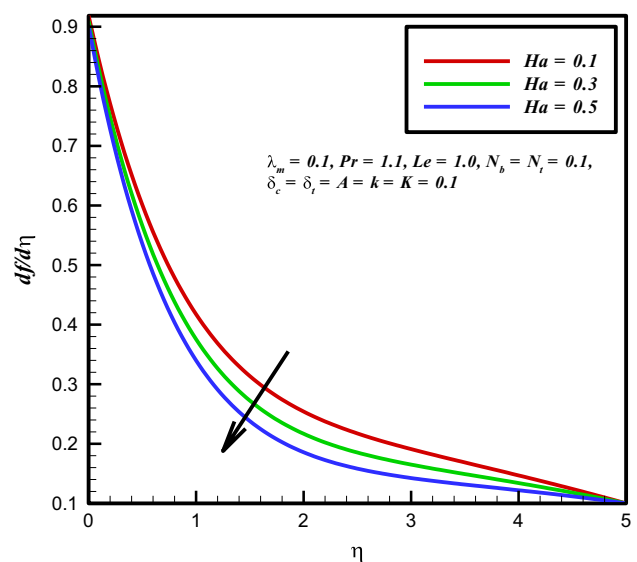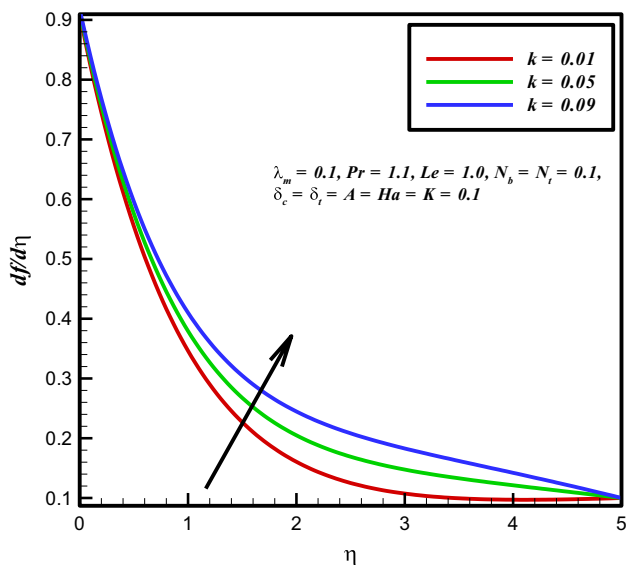

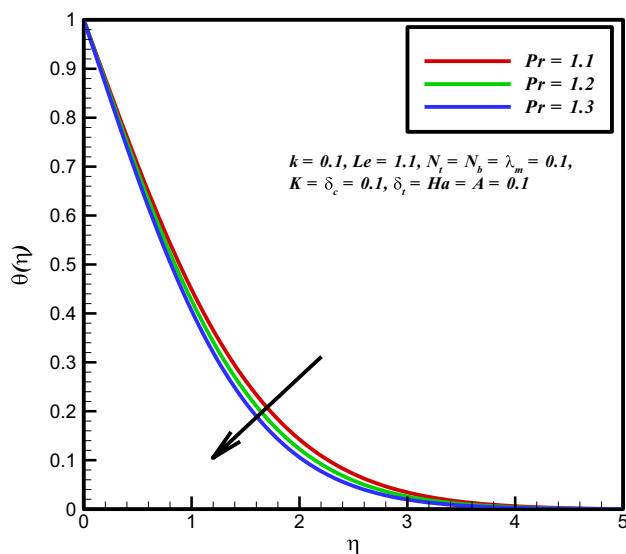**Fig. 2** Outcome of Ha on $f'(\eta)$

Fig. 3 Outcome of k on $f'(\eta)$

Fig. 5 Outcome of Pr on $\theta(\eta)$

Fig. 4 Outcome of λ_m on $f'(\eta)$
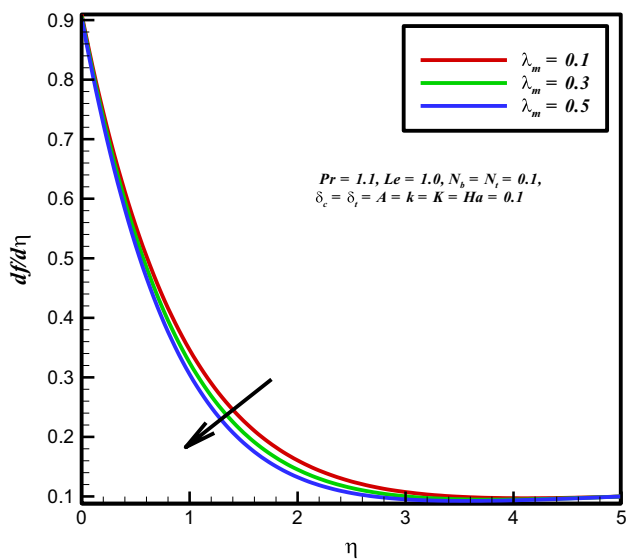

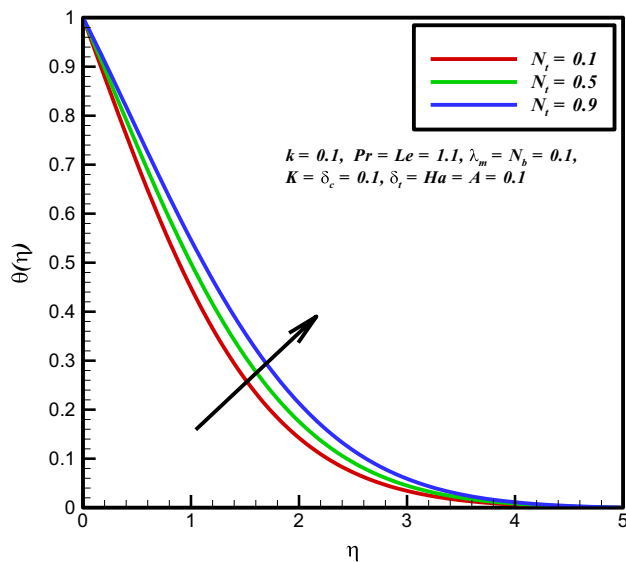**Fig. 6** Outcome of N_b on $\theta(\eta)$

the boundary layer thickness. Figure 7 shows the behavior of Prandtl number Pr on temperature profile. It is found that the temperature profile reduces with rising values of Prandtl Pr. Figure 8 presents the deviation of temperature profile for distinct values of δ_t. It is seen that by enhancing thermal relaxation parameter δ_t, fluid

particles require more time to heat the boundary layer region, and as a result temperature profile reduces. Figure 9 displays the effect of relaxation parameter δ_c on concentration distribution. From this figure, it is observed that by increasing the relaxation parameter δ_t, the concentration profile reduces. Figure 10 represents the variation
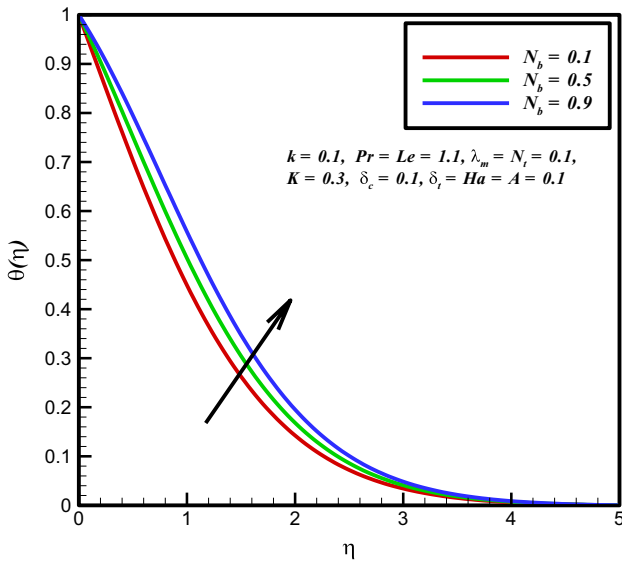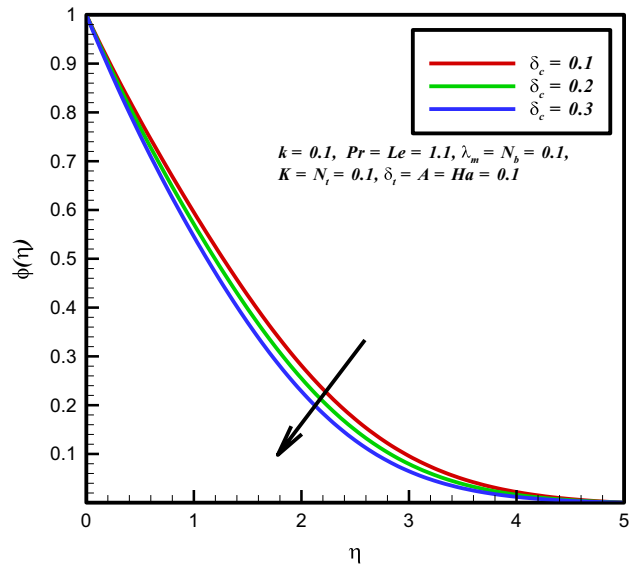
Fig. 7 Outcome of N_t on $\theta(\eta)$

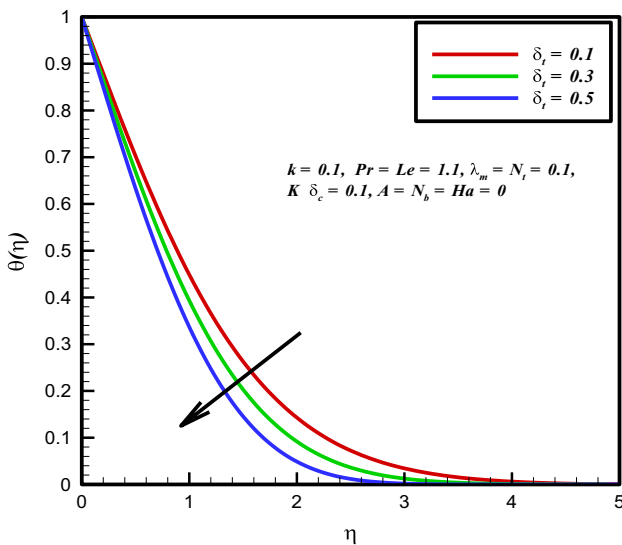**Fig. 9** Outcome of δ_t on $\phi(\eta)$

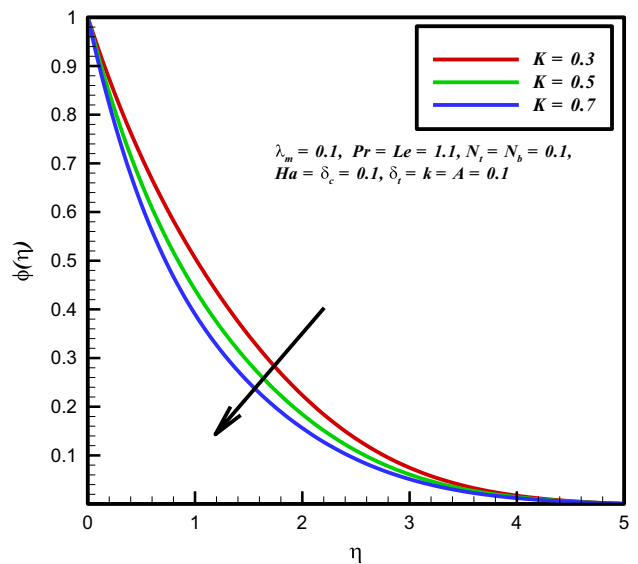**Fig. 8** Outcome of δ_t on $\theta(\eta)$

Fig. 10 Outcome of K on $\phi(\eta)$

on concentration profile for different values of chemical reaction K. It is found that for large values of chemical reaction K reduces the concentration profile. Figure 11 represents the influence of Lewis number Le on nano-concentration profile. It is found that the higher values of Lewis number Le lead to reduction in the mass diffusivity, so the concentration profile reduces. Figures 12 and 13 validate the distribution of skin friction coefficient $C_f Re_x^2$ with respect to Hartmann number Ha and

for several values of slip parameter k and fluid relaxation parameter λ_m. It is very important to see that the skin friction coefficient $C_f Re_x^2$ enhances by enhancing slip parameter k but decreases by increasing the fluid relaxation parameter λ_m. Table 1 shows that the fraction factor rises due to an increase in Hartmann number Ha and fluid relaxation parameter λ_m and opposite behavior is noticed for slip parameter k. The achieved results are in
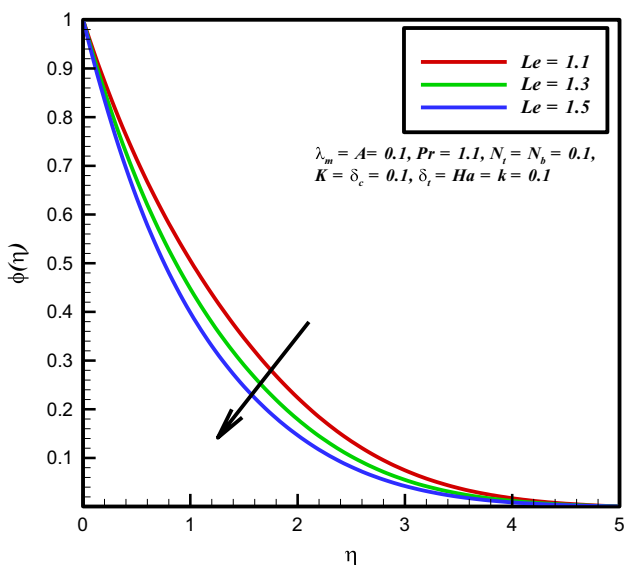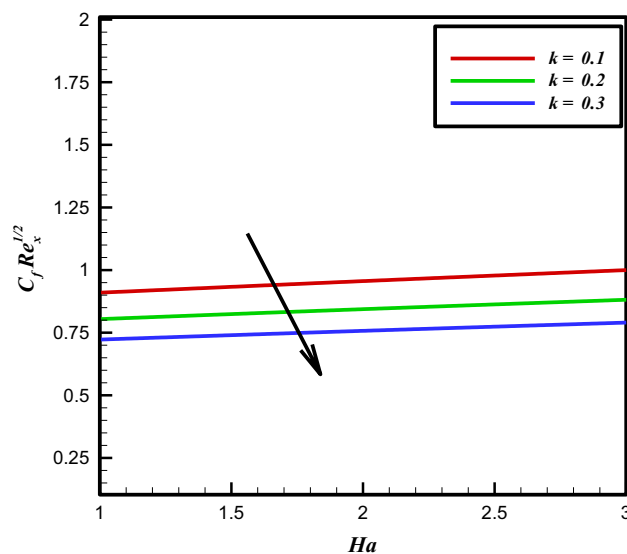
Fig. 11 Outcome of Le on $\phi(\eta)$

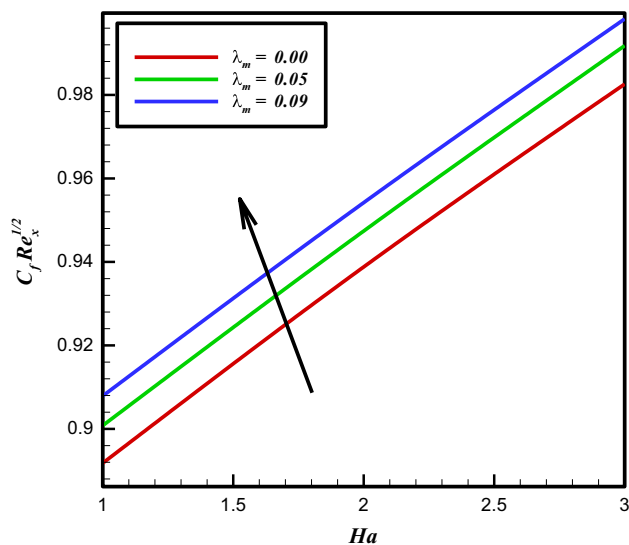**Fig. 13** $C_f Re_x^{\frac{1}{2}}$ for various values of Ha and k

Fig. 12 $C_f Re_x^{\frac{1}{2}}$ for various values of Ha and λ_m

Table 1 Computational results of $C_f Re_x^{\frac{1}{2}}$ for different values of Ha, k and λ_m when $K = A = N_b = 0.1$, $Le = 1.0$, $\delta_c = \delta_t = 0.0$, $N_t = 0.5$, and $Pr = 1.1$

Ha	k	λ_m	$-C_f Re_x^{\frac{1}{2}}$
0.1		0.1	0.9097
0.2			0.9559
0.3			0.9999
	0.1		0.9097
	0.2		0.8042
	0.3		0.7225
		0.00	0.8918
		0.05	0.9008
		0.09	0.9097

Table 2 Comparison of $(f''(0) + \lambda_m(f'(0)f''(0) + f(0)f'''(0)))$ with the previous literature when $N_b = k = St = 0.1$, $\delta t = \delta c = K = A = 0.0$, $N_t = 0.5$ and $Le = Pr = 1.0$

λ_m	Ha	[25]	Present results
0.5	0.0	-1.68935	-1.6752
0.5	0.1	-1.69715	-1.6821
0.5	0.2	-1.72034	-1.7000
0.5	0.3	-1.75830	-1.7321
0.0	0.1	-1.00499	-1.0001
0.1	0.1	-2.49440	-2.1898

good agreement with Afify and Elgazery [25] for different values Ha and λ_m as shown in Table 2. Table 3 is sketched for the comparative investigation between Hsiao [26] and present results. $N_t N_b = 0.1$, $Le = Pr = 10$ and $\lambda_m = Ha = k = St = \delta t = \delta c = K = A = 0.0$.

Table 3 Comparison of $-\theta'(0)$ and $-\phi'(0)$ with the previous literature when $\lambda_m = Ha = k = St = \delta t = \delta c = K = A = 0.0$, $N_t = 0.1$ and $Le = Pr = 10$

N_t	Hsiao [26]	Hsiao [26]	Present outcome	Present outcome
0.1	-0.9524	-2.1294	-0.9131	-2.1526
0.2	-0.6932	-2.2740	-0.6922	-2.2945
0.3	-0.5201	-2.5287	-0.5018	-2.5002
0.4	-0.4026	-2.7952	-0.4022	-2.7590
0.5	-0.3211	-3.0352	-0.3462	-3.0617

5 Conclusions

The main results for heat and mass exchanger in MHD stagnation point Maxwell nanofluid flow past a linear stretching surface in the presence of slip effects are summarized below:

- Rising the Hartmann number Ha and slip parameter k leads to decline in velocity profile.
- Larger values of fluid relaxation parameter λ_m, increase the velocity profile.
- For increasing values of chemical reaction, K, Prandtl number Pr, thermal relaxation parameter δ_t, concentration relaxation parameter δ_c and Lewis number Le reduce the concentration and temperature profiles.
- Temperature profile increases for increasing values of thermophoresis parameter N_t and Brownian motion N_b.
- Skin friction coefficient reduces $C_f\,Re_x^{\frac{1}{2}}$ for large values of slip parameter k but opposing behavior is noticed for fluid relaxation parameter λ_m.

Compliance with ethical standards

References

1. Choi SUS (1995) Enhancing thermal conductivity of fluids with nanoparticles. In: Proceedings of the ASME international mechanical engineering congress and exposition, San Francisco, Calif, USA, vol 66, pp 99–105
2. Rundora L, Makinde OD (2015) Effects of Navier slip on unsteady flow of a reactive variable viscosity non-Newtonian fluid through a porous saturated medium with asymmetric convective boundary conditions. J Hydrodyn 27:934–944
3. Babu MJ, Sandeep N (2016) Three-dimensional MHD slip flow of nanofluids over a slendering stretching sheet with thermophoresis and Brownian motion effect. Adv Powder Technol 27:2029–2050
4. Hsiao KL (2017) Micropolar nanofluid flow with MHD and viscous dissipation effects towards a stretching sheet with multimedia feature. Int J Heat Mass Transf 112:983–990
5. Mahdavi M, Sharifpur M, Meyer JP (2017) Implementation of diffusion and electrostatic forces to produce a new slip velocity in the multiphase approach to nanofluids. Powder Technol 307:153–162
6. Xun S, Zhao J, Zheng L, Zhang X (2017) Bioconvection in rotating system immersed in nanofluid with temperature dependent viscosity and thermal conductivity. Int J Heat Mass Transf 111:1001–1006
7. Khan M, Shahid A, Malik MY, Salahuddin T (2018) Thermal and concentration diffusion in Jeffery nanofluid flow over an inclined stretching sheet: a generalized Fourier's and Fick's perspective. J Mol Liq 251:7–14
8. Lebon G, Machrafi H (2018) A thermodynamic model of nanofluid viscosity based on a generalized Maxwell-type constitutive equation. J Nonnewton Fluid Mech 253:1–6
9. Ansari HR, Zarei MJ, Sabbaghi S, Keshavarz P (2018) A new comprehensive model for relative viscosity of various nanofluids using feed-forward back-propagation MLP neural networks. Int Commun Heat Mass Transf 91:158–164
10. Khan M, Shahid A, Malik MY, Salahuddin T (2018) Chemical reaction for Carreau-Yasuda nanofluid flow past a nonlinear stretching sheet considering Joule heating. Results Phys 8:1124–1130
11. Zhao J, Zheng L, Zhang X, Liu F (2016) Convection heat and mass transfer of fractional MHD Maxwell fluid in a porous medium with Soret and Dufour effects. Int J Heat Mass Transfer 103:203–210
12. Hsaio KL (2017) Combined electrical MHD heat transfer thermal extrusion system using Maxwell fluid with radiative and viscous dissipation effects. Appl Therm Eng 112:1281–1288
13. Ghasemi K, Siavashi M (2017) MHD nanofluid free convection and entropy generation in porous enclosures with different conductivity ratios. J Magn Magn Mater 442:474–490
14. Nourazar SS, Hatami M, Ganji DD, Khazayinejad M (2017) Thermal-flow boundary layer analysis of nanofluid over a porous stretching cylinder under the magnetic field effect. Powder Technol 317:310–319
15. Dogonchi AS, Ganji DD (2017) Impact of Cattaneo–Christov heat flux on MHD nanofluid flow and heat transfer between parallel plates considering thermal radiation effect. J Taiwan Inst Chem Eng 80:52–63
16. Hayat T, Khalid H, Waqas M, Alsaedi A, Ayub M (2017) Homotopic solutions for stagnation point flow of third-grade nanoliquid subject to magnetohydrodynamics. Results Phys 7:4310–4317
17. Sayyed R, Singh BB, Bano N (2018) Analytical solution of MHD slip flow past a constant wedge within a porous medium using DTM-Padé. Appl Math Comput 321:472–482
18. Khan M, Salahuddin T, Malik MY (2018) An immediate change in viscosity of Carreau nanofluid due to double stratified medium:

application of Fourier's and Fick's laws. J Braz Soc Mech Sci Eng 40(9):457

19. Khan M, Shahid A, Salahuddin T, Malik MY, Mushtaq M (2018) Heat and mass diffusions for Casson nanofluid flow over a stretching surface with variable viscosity and convective boundary conditions. J Braz Soc Mech Sci Eng 40(11):533. https://doi.org/10.1007/s40430-018-1415-y

20. Hayat T, Khan MI, Farooq M, Alsaedi A, Waqas M, Yasmeen T (2016) Impact of Cattaneo–Christov heat flux model in flow of variable thermal conductivity fluid over a variable thicked surface. Int J Heat Mass Transf 99:702–710

21. Nadeem S, Haq RU, Khan ZH (2014) Numerical study of MHD boundary layer flow of a Maxwell fluid past a stretching sheet in the presence of nanoparticles. J Taiwan Inst Chem Eng 45:121–126

22. Reddy PB, Suneetha S, Reddy NB (2017) Numerical study of magnetohydrodynamics (MHD) boundary layer slip flow of a Maxwell nanofluid over an exponentially stretching surface with convective boundary condition. Propuls Power Res 6(4):259–268

23. Liu L, Liu F (2018) Boundary layer flow of fractional Maxwell fluid over a stretching sheet with variable thickness. Appl Math Lett 78:92–98

24. Yang X, Qi H, Jiang X (2018) Numerical analysis for electroosmotic flow of fractional Maxwell fluids. Appl Math Lett 78:1–8

25. Afify AA, Elgazery NS (2016) Effect of a chemical reaction on magnetohydrodynamic boundary layer flow of a Maxwell fluid over a stretching sheet with nanoparticles. Particuology 29:154–161

26. Hsiao KL (2016) Stagnation electrical MHD nanofluid mixed convection with slip boundary on a stretching sheet. Appl Therm Eng 98:850–861. https://doi.org/10.1016/j.applthermaleng.2015.12.138